Expanded Austenite Formation on Stainless Steel via Nitrogen/Hydrogen Atmospheric-Pressure Thermal Plasma Jet

Ryuta ICHIKI*, Takashi FURUKI, Seiji KANAZAWA

Oita University, Oita 870-1192, Japan

(Received 23 March 2026 / Accepted 18 May 2026)

Surface layers of expanded austenite (S-phase) are formed on JIS SUS304 austenitic stainless steel by nitrogen doping using a pulsed-arc plasma jet under atmospheric pressure. The characteristics of the formed S-phase strongly depend on the fraction of hydrogen gas in the operating nitrogen/hydrogen gas mixture, i.e., plasma nitriding with a higher hydrogen fraction provides a more uniform but thinner S-phase. Conversely, reductive pretreatment using a high hydrogen fraction prior to nitrogen doping affords a thicker S-phase while maintaining uniformity.

Keywords: atmospheric-pressure plasma jet, expanded austenite, stainless steel, nitrogen doping, reductive method

DOI: 10.1585/pfr.21.1306041

Austenitic stainless steels are corrosion-resistant and widely used in various industries, especially in food processing equipment and chemical plants. However, their wide-scale structural applications are hindered by their low hardness and poor wear resistance. Expanded austenite, also known as the S-phase, formed on the surface of austenitic stainless steels, has been actively studied to overcome this shortcoming [1–10]. The S-phase contains supersaturated nitrogen, which distorts and expands the lattice structure of austenite, leading to high surface hardness and good wear resistance. The S-phase can be produced using reactive plasma to introduce nitrogen atoms into the material surface via thermal diffusion. Notably, the passive film on the stainless-steel surface, which confers good corrosion resistance, must be removed before or during nitrogen doping because it acts as a barrier against nitrogen penetration through the surface [6]. Generally, ion sputtering is effective for passive film removal in typical low-pressure plasma-nitriding techniques such as ion nitriding [1, 3, 4, 7] and active-screen plasma nitriding [2, 9, 10]. Additionally, the nitrogen must be doped at a temperature lower than the precipitation temperature of ca. 723 K to avoid the degradation of the corrosion resistance of stainless steels [6].

Previously, we developed a unique plasma-nitriding technique using atmospheric-pressure plasma [11–16]. This technique employs a thermal plasma jet onto the target material's surface. Nitrogen atoms formed via plasma chemical reactions penetrate the sprayed material surface. This technique has been used for nitrogen doping to hot-work steels [11, 15], cold-roll steels [14], titanium alloys [12, 13], and diamond electrodes [16]. Such atmospheric-pressure plasma nitriding does not require vacuum equipment, thereby reducing working hours and capital costs. However, the treatable range is limited to a diameter of 20 mm [11–15]. For these reasons, this technique is a potential candidate for a novel nitriding technique specialized in high-mix, low-volume fabrication suggested in Society 5.0 [17]. However, the ion-sputtering effect is not induced at atmospheric pressure because the mean free path of the ions is too short. Therefore, in this study, we leverage hydrogen's reductive effect to remove the passive film from stainless steel to induce the S-phase formation at atmospheric pressure.

Figure 1 presents a schematic of the nitriding system with the pulsed-arc plasma jet. The jet nozzle comprises coaxial cylindrical electrodes. The external electrode with an inner diameter of 35 mm is grounded. The operating gas is a nitrogen/hydrogen gas mixture, which bleeds into the jet nozzle through two separate mass flow controllers (HORIBA STEC, SEC series) at a total flow rate of 20 slm (standard liter per minute). Here, f is the hydrogen fraction in the operating gas, controlled in the range from 0 to 0.05. Low-frequency voltage pulses of ca. 5-kV height with a 21-kHz repetition are applied to the inner electrode using a high-voltage power supply (plasmatreat FG3001), generating pulsed-arc discharges of ca. 1.2 A between the discharge gap of ca. 20 mm. Afterglow is spewed out from the orifice of 4-mm diameter, forming a jet plume.

For the nitriding treatment, the jet nozzle is inserted into the cylindrical quartz cover of the nitriding chamber (Fig. 1) to purge residual oxygen from the treatment atmosphere. The quartz cover has a height and diameter of 85 and 124 mm, respectively. The gas is exhausted through a 0.5-mm gap between the jet nozzle and quartz cover. Before generating the plasma jet, residual oxygen inside the cover is gas-purged by the operating gas introduced through the nozzle.

Circular disks of austenitic stainless steel JIS SUS304,

*Corresponding author's e-mail: ryu-ichiki@oita-u.ac.jp

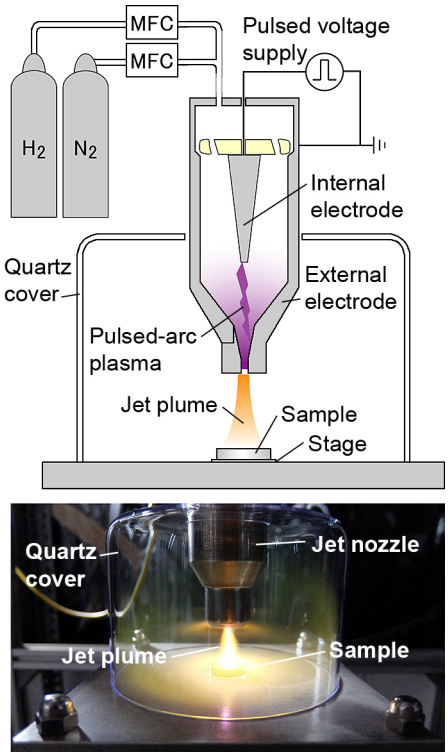

Fig. 1. Schematic (above) and photograph (below) of plasma-jet nitriding system. MFC represents a mass flow controller.

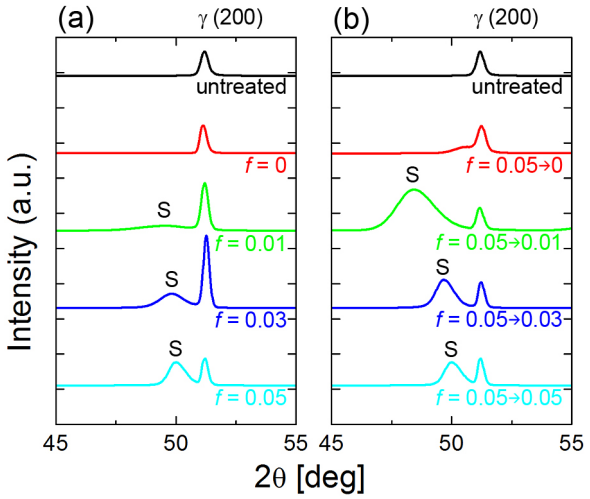

Fig. 2. XRD pattern of the sample surface (a) treated using several fixed hydrogen fractions *f* and (b) high-*f* pretreatment. (The spectrum of *f* = 0.05 → 0.05 in (b) is reproduced from that of *f* = 0.05 in (a)).

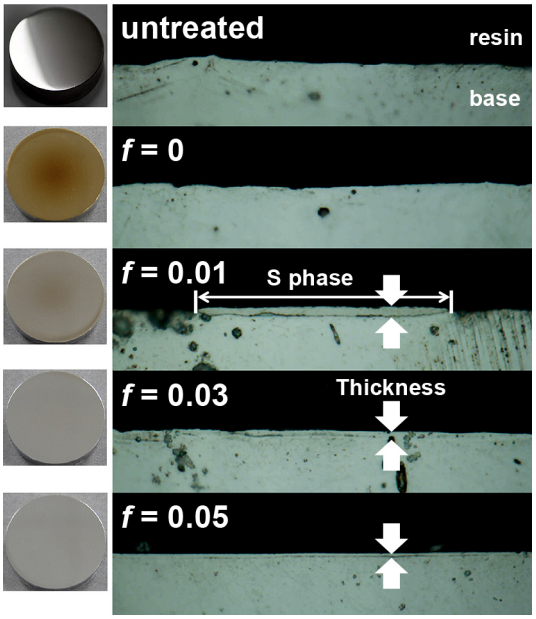

Fig. 3. Mettalographic structure of the sample cross-section for several fixed hydrogen fractions *f*.

20 mm in diameter and 4 mm in thickness, are used as samples for nitrogen doping. The surface is mirror-finished with alumina powder and degreased in an ultrasonic acetone bath. The sample is placed on the quartz stage inside the quartz cover.

Nitrogen doping is performed by spraying the sample surface with the jet plume. The treatment temperature of ca. 690 K is maintained by the plasma-jet spraying, where the distance between the nozzle tip and the surface is 35 mm. The treatment temperature is measured using a dummy sample with a thermocouple fitted on the surface. The treatment duration is 7.2 ks. The crystal phase of the sample surface is analyzed by X-ray diffraction (XRD, RIGAKU SmartLab) using Cu Kα radiation. The metallographic microstructure is observed using an optical microscope (KEYENCE VHX-5000), where the sample cross-section is pre-etched by aqua regia.

Figure 2(a) shows XRD patterns of the sample surface treated at several *f* values. The spectral peak γ corresponds to the (200) plane of the original austenitic phase. The γ peak only appears for *f* = 0. Another broader peak S appears at a lower 2θ for finite *f*. According to previous studies [3, 6, 9, 10], the appearance of S indicates the S-phase formation. Note that the 2θ position at which S appears gradually increases with increasing *f*, indicating that the nitrogen concentration in the formed S-phase decreases with increasing *f* [6]. The expansion ratio of the lattice parameter, calculated from the shift in the diffraction angle, is 2.4%, 2.1%, and 1.7% for *f* = 0.01, 0.03, and 0.05, respectively. This tendency is consistent with the known property of plasma-jet nitriding, i.e., amount of nitrogen dopant decreases with increasing *f* within the range from 0.01 to 0.05 [11, 15]. Note that the intensity of S increases with increasing *f*, as discussed in the following paragraph.

Figure 3 shows the metallographic microstructure of the sample cross-section in the vicinity of the outermost surface. No surface layer is found for *f* = 0. In contrast, a discontinuous surface layer is formed for finite *f*. Because the *f*-dependence is consistent with that of S in the XRD spectra, we conclude that the discontinuous layer is the S-phase.

Note that this layer formation strongly depends on *f*. First, increasing *f* leads to a uniform layer. The surface layer is formed only partially for *f* = 0.01. In the metallographic structure, the coverage of this layer is ca. 60%, and similar nonuniformity is observed across the sample surface. For *f* = 0.03, the coverage increases to ca. 100%; however, the layer thick-

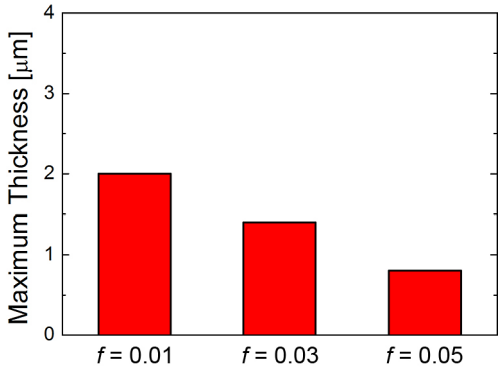

Fig. 4. Maximum thickness of the S-phase formed on the sample for several fixed hydrogen fractions *f*.

ness still appears nonuniform. For $f = 0.05$, the layer thickness becomes quite uniform. This uniformity trend can be explained as follows: First, increasing f enhances the reductive ability of the plasma, leading to better removal of the original passive layer on the stainless steel, resulting in a uniform S-phase formation. In addition, the intensity trend of S (Fig. 2(a)) may reflect the uniformity trend. Second, increasing f leads to a thinner layer formation. Figure 4 shows the maximum thickness of the formed surface layer. The maximum thickness is as high as ca. 2.0 μm for $f = 0.01$, although the layer is quite nonuniform. However, the thickness tends to decrease to ca. 1.4 and 0.8 μm with increase in f up to 0.03 and 0.05, respectively. This thickness trend is consistent with the abovementioned property of plasma-jet nitriding, wherein the amount of nitrogen dopant decreases as f increases.

In summary, the S-phase is successfully formed with atmospheric-pressure plasma nitriding; however, the layer's quality is not ideal, i.e., to form a thick S-phase, f should decrease, but the layer becomes nonuniform. Conversely, to form a uniform S-phase, f should increase, but the thickness decreases. Thus, there is a tradeoff between forming a thick or uniform S-phase. We expect that the loss of uniformity upon decreasing f is attributed to the degraded reductive ability of the plasma, based on the fact that its reductive ability has been found to increase with f for steel surfaces without passive layers [15]. Thus, we attempt to overcome the degraded uniformity by improving the reductive method.

As an improved method, we attempt maximal removal of the passive layer in the initial stage of nitriding by setting the initial f to a high value of 0.05. The duration of the high-f pretreatment is 1.8 ks. After the pretreatment, the f value is decreased to 0, 0.01, or 0.03 to vary the amount of nitrogen dopant. The total treatment duration is 7.2 ks, including the high-f pretreatment.

Figure 2(b) shows XRD patterns of the sample surface nitrided via the high-f pretreatment. S does not appear for $f = 0$, possibly because the amount of nitrogen dopant in the high-f pretreatment is not enough to form a considerable amount of the S-phase. Conversely, S appears for $f = 0.01$ and 0.03. Note that the spectral intensity of this peak is considerably greater than in Fig. 2(a). Figure 5 shows the metallographic

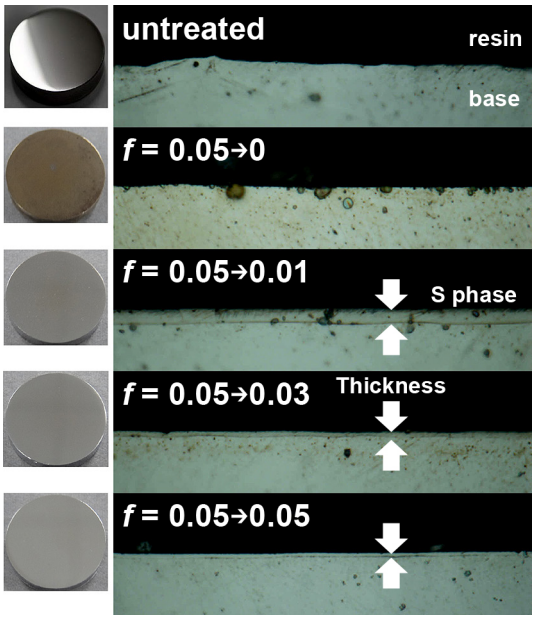

Fig. 5. Mettalographic structure of the sample cross-section treated with high-f pretreatment. (The photograph of $f = 0.05 \rightarrow 0.05$ is reproduced from that of $f = 0.05$ in Fig. 3).

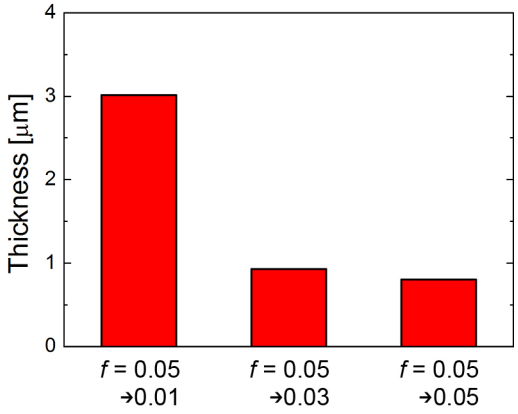

Fig. 6. Average thickness of the S-phase formed on the sample treated with high-f pretreatment. (The bar of $f = 0.05 \rightarrow 0.05$ is reproduced from that of $f = 0.05$ in Fig. 4).

microstructure of the sample cross-section subjected to high-f pretreatment. First, the thickness of the S-phase is uniform for $f = 0.01$ and 0.03 compared with that in Fig. 3. The success in improving the layer uniformity by the high-f pretreatment is consistent with our expectation that the layer uniformity depends on the initial removal of the original passive layer. Figure 6 shows the average thickness of the S-phase. Note that the layer thickness for $f = 0.01$ increases from 2.0 to 3.0 μm upon pretreatment, in conjunction with the uniformity improvement, possibly caused by smooth nitrogen doping of the sample surface without the passive layer. Moreover, the pretreatment increased the expansion ratio of the lattice parameter to 4.1 and 2.3% for $f = 0.01$ and 0.03, respectively.

In summary, we aim to form a uniform and thick S-phase using an atmospheric-pressure plasma jet to provide a practical case-hardening technique for high-mix, low-volume stainless-

steel components. Here, the original passive layer on the sample surface must be removed by leveraging the reductive ability of hydrogen because the ion-sputtering effect is not operative under atmospheric pressure. First, the hydrogen fraction f is fixed during plasma nitriding. This leads to tradeoff between layer uniformity and thickness: the formed S-phase is uniform (nonuniform) but thin (thick) for high (low) f. This contradiction limits the S-phase thickness to 0.8 μm when maintaining the layer uniformity. We expect that the uniformity degradation is attributed to the degraded reductive ability of the plasma. For this reason, we introduce a high-f pretreatment to remove the passive layer in the initial stage of the treatment, achieving a uniform S-phase as thick as 3.0 μm upon treatment for 7.2 ks.

In comparison, Tsujikawa *et al.* obtained ca. 6-μm thick S-phase on SUS304 via typical ion nitriding for 28.8 ks [3]. In addition, Hamashima and Nishimoto obtained a 3.6-μm thick S-phase via active-screen plasma nitriding for 18 ks [9]. According to diffusion theory [12], these treatments yield an S-phase with thicknesses of 3 and 2.3 μm, respectively, assuming a treatment duration of 7.2 ks. Based on this estimation, plasma-jet nitriding should be as effective as conventional low-pressure plasma-nitriding techniques for S-phase formation in terms of layer thickness. However, the maximum obtained expansion ratio of the S(200) plane is ca. 4.1% in plasma-jet nitriding for 7.2 ks, while Kuribayashi and Nishimoto obtained ratios more than 6% although employing a longer treatment duration than in this study [10]. In any case, we need to examine the effect of the amount of nitrogen dopant in more detail. Future research will focus on experimental validation of the f-dependence of passive layer removal.

We are grateful to Prof. H. Nishiguchi, A. Maeda, R. Otani, and K. Nakahara of Oita University, and Dr. M. Sonoda of Oita Industrial Research Institute for their valuable assistance. This work was supported by JSPS KAKENHI Grant Numbers 20H02133 and 24K00871.

[1] E. Menthe *et al.*, Surf. Coat. Technol. **133**, 259 (2000).
[2] C.X. Li and T. Bell, Corros. Sci. **46**, 1527 (2004).
[3] M. Tsujikawa *et al.*, Mater. Trans. **46**, 863 (2005).
[4] F. Borgioli *et al.*, Surf. Coat. Technol. **200**, 5505 (2006).
[5] L.C. Gontijo *et al.*, Surf. Eng. **26**, 265 (2010).
[6] L.C. Casteletti *et al.*, Metallogr. Microstruct. Anal. **3**, 477 (2014).
[7] E. de Araújo Jr. *et al.*, J. Mater. Res. Technol. **8**, 2180 (2019).
[8] L.A. Luiz *et al.*, Mater. Today Commun. **28**, 102655 (2021).
[9] S. Hamashima and A. Nishimoto, Mater. Trans. **63**, 1170 (2022).
[10] M. Kuribayashi and A. Nishimoto, NETSU SHORI **64** Extra edition, 60 (2024).
[11] H. Nagamatsu *et al.*, Surf. Coat. Technol. **225**, 26 (2013).
[12] Y. Yoshimitsu *et al.*, Jpn. J. Appl. Phys. **54**, 030302 (2015).
[13] R. Sannomiya *et al.*, Plasma Fusion Res. **13**, 1306120 (2018).
[14] R. Ichiki *et al.*, Metals **9**, 714 (2019).
[15] K. Toda *et al.*, Jpn. J. Appl. Phys. **59**, SHHE01 (2020).
[16] T. Kinumoto *et al.*, Electrochemistry **91**, 057002 (2023).
[17] K. Yamamoto, J. IEIE Jpn. **39**, 477 (2019). [in Japanese]